Journal Pre-proofs

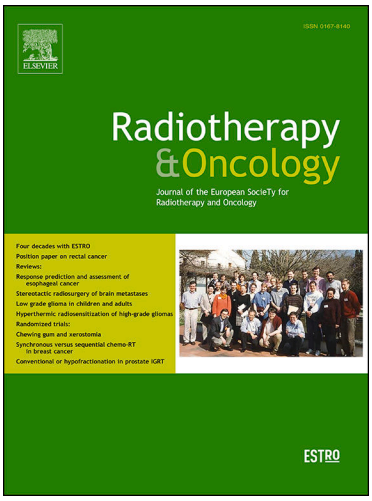

Original Article

Pencil beam scanning proton therapy for the treatment of craniopharyngioma complicated with radiation-induced cerebral vasculopathies: a dosimetric and linear energy transfer (LET) evaluation

Alessandra Bolsi, Lorenzo Placidi, Alessia Pica, Frank Ahllhelm, Marc Walser, Tony Lomax, Damien C. Weber

PII: S0167-8140(20)30233-4
DOI: https://doi.org/10.1016/j.radonc.2020.04.052
Reference: RADION 8303

To appear in: *Radiotherapy and Oncology*

Received Date: 22 May 2019
Revised Date: 27 April 2020
Accepted Date: 28 April 2020

Please cite this article as: Bolsi, A., Placidi, L., Pica, A., Ahllhelm, F., Walser, M., Lomax, T., Weber, D.C., Pencil beam scanning proton therapy for the treatment of craniopharyngioma complicated with radiation-induced cerebral vasculopathies: a dosimetric and linear energy transfer (LET) evaluation, *Radiotherapy and Oncology* (2020), doi: https://doi.org/10.1016/j.radonc.2020.04.052

Pencil beam scanning proton therapy for the treatment of craniopharyngioma complicated with radiation-induced cerebral vasculopathies: a dosimetric and linear energy transfer (LET) evaluation

Alessandra Bolsi[1*], Lorenzo Placidi[2*], Alessia Pica[1], Frank Ahllhelm[3], Marc Walser[1], Tony Lomax[1,4], Damien C. Weber[1,5,6]

*Equally contributed to this manuscript

[1]Center for Proton Therapy, Paul Scherrer Institute, ETH Domain, CH-5232 Villigen, Switzerland
[2]Fondazione Policlinico Universitario A. Gemelli IRCCS, Roma - Università Cattolica del Sacro Cuore, Rome, Italy
[3]Department of Radiology, Cantonal Hospital Baden, CH-5404 Baden, Switzerland
[4]ETH Zürich, Rämistrasse 101, 8092 Zürich, Switzerland
[5] Department of Radiation Oncology, University Hospital of Zürich, Zürich, CH-8000, Switzerland
[6] Department of Radiation Oncology, University Hospital of Bern, Bern, CH-3010, Switzerland

Corresponding author:

Alessandra Bolsi
Head clinical medical physics group
Center for Proton Therapy, CPT
Paul Scherrer Institute, ETH Domain
5232 Villigen
SWITZERLAND
Email: alessandra.bolsi@psi.ch

Conflicts of Interest Notification: none. The content of the manuscript has not been published or submitted for publication elsewhere.

Word counting (Abstract):	2995 (249)
Figures (Tables):	4 (2)
Supplementary Tables(Figures):	1(1)
Appendix:	1

Running Title: Vascular toxicity after proton therapy for craniopharyngioma: a dosimetric and LET evaluation.

Key words: craniopharyngioma radiation-induced complication; vasculopathy; linear energy transfer; pencil beam scanning proton therapy; children.

Acknowledgments:

We thank Anna Wiener Wellauer and Beate Schulz for providing data management, Dr Ralf Schneider and Dr. Gudrun Goitein for treating these patients and for providing data entry.

Abstract

Background and Purpose. This study analyses the dosimetric and dose averaged Linear Energy transfer (LETd) correlation in paediatric craniopharyngioma (CP) patients with and without radiation-induced cerebral vasculopathies (RICVs) treated with pencil beam scanning (PBS) proton therapy (PT).

Material and Methods. We reviewed a series of 16 CP patients treated with PT to a median dose of 54 Gy(RBE). Two (12.5%) index patients presented RICVs 14 and 24 months (median, 19) after PT. Organs at risks (OARs) as bilateral internal carotid arteries (ICAs) and circle of Willis were contoured based on CTs and MRIs pre- and post-PT. Dosimetry was reviewed and LETd distributions were calculated; LETd metric for PTVs and OARs were analysed. For a sub-cohort, dosimetric and LETd values robustness due to range uncertainties were computed.

Results.

For the two index patients, no correlation was observed between RICVs and OARs doses. However for those patients mean(*maximum*) LETd values in the affected OARs were up to 4.0±0.4 (*7.8±0.1*)keV/μm; those LETd values were significantly higher (p=0.02) than the mean(*maximum*) LETd values for the rest of the cohort (mean: 3.1±0.3, *maximum: 4.8±1.0*keV/μm). This was due to asymmetric field arrangement, thus resulting in marked asymmetric LETd distributions. For such arrangement, maximum LETd values variations in vascular structures due to range uncertainties were up to 1.2keV/μm, whilst for the symmetric one they were up to 0.7keV/μm.

Conclusions. For children with and without RICVs, quantitative analysis showed a significant correlation with LETd average/maximum values in vascular structures, whilst no correlation was found on dosimetric parameters.

Introduction

Radiation-induced cerebral vasculopathy (RICV) has been described in paediatric patients after radiation therapy (RT) for tumours of optic tracts, hypothalamus, and suprasellar region [1, 2]. Delayed RICV mainly results from an accelerated arteriosclerosis process of small and medium sized vessels within the radiation field [3, 4]. This complication can present as *moyamoya* syndrome, which results from stenosis or occlusion of large and intermediate cerebral arteries [5]. The real incidence of RT-induced stenosis of carotid arteries and intracerebral arteries is however not well established. It seems that the vasculature of young children, when compared to adult patients, is more radio-sensitive to vasculature damage. In one report, *moyamoya* syndrome after RT has been observed most commonly in children <5 years of age receiving RT to the suprasellar region [6]. The Circle of Willis is often located in high dose region (≥ 45Gy) in the irradiation of suprasellar tumors; however the development of *moyamoya* syndrome seems to be independent from the radiation delivered to vascular structure and may result from pre-irradiation compressive vasculopathy and manipulation of vessels during surgeries [6, 7]. Craniopharyngiomas (CPs) are rare epithelial tumours arising along the path of the craniopharyngeal duct located in the suprasellar region. Despite their non-infiltrative growth pattern, their adherence/compression to nearby critical organs at risk (OARs) makes the treatment challenging. As such, radiation-induced complications, including but not limited to pituitary dysfunction, cognitive deficits, visual impairment and brain necrosis have been reported. Importantly, late effects on the vasculature, such as cavernomas or hemangiomas [8, 9], has been observed not infrequently. The superior dose profile and distribution provided by proton therapy (PT) may contribute to a reduced exposure of normal tissue, including blood vessels. The relative biological effectiveness of protons (RBE), approximated to be constant and equal to 1.1. RBE, depends however on physical properties,

such as the Linear Energy Transfer (LET) and dose per fraction, as well as biological properties including cell type and clinical endpoint. Moreover, LET and consequently RBE value increases at the end of the proton beam range [10]: this could translate into a potential increase of toxicity of normal tissue within and immediately adjacent to the region of elevated RBE-weighted dose.

In this study, we propose a) to report two cases of RICV after PBS PT for pediatric CP patients, b) to assess the dosimetry of plans delivered to CP patients with or without RICV and c) to evaluate dose-averaged linear energy transfer (LETd) distributions for all the patients and its intrinsic uncertainty with special focus on these RICVs.

Materials and Methods

Patients' cohort and clinical outcome

Sixteen paediatric patients treated for CP with PBS PT from 2008 to 2014 with >1 year of follow-up were identified from the Paul Scherrer Institute's institutional database. Median age was 9.5 years (range, 2.0 – 18.2), 63% of the patients were female. Thirteen (81%) patients had hypopituitarism and 12 (75%) had a visual defect prior to PT, respectively. PT was administered for progressive disease after surgical resection (n=13; 81%) or postoperatively after partial resection (n=3; 19%). Median time from diagnosis to delivery of PT ranged from 4.0 months to 8.8 years (median, 13.0 months). A dose of 54.0 Gy Relative Biological Equivalent (Gy(RBE)) was delivered at 1.8 Gy(RBE) per fraction, five times per week. The planning- (PTV) and clinical- (CTV) target volume median values were 43.0 cm^3 (range 11.6-159.8) and 24.4 cm^3 (range 5.8-88.5) respectively. PTV was generated as a 5 mm isotropic CTV expansion.

Institutional review board-approval was obtained to analyse retrospectively the treatment-related toxicity of PT of these patients (EKNZ 2015-423).

Two out of 16 patients (12.5%), showed RICV 1.2 and 2 years after PT (indicated as index patients). One 5-year-old patient with toxicity, (patient A), received PT 7 months after the initial diagnosis and multiple cyst aspirations in two surgical procedures. Two years after irradiation, she developed several transient ischaemic attacks (TIAs) with a right facial paresis. The MRI revealed a small mid-left infarct and progressive multifocal RICVs in the region of the circle of Willis (Fig. 1b). She is currently taking aspirin for anticoagulation. The other index patient was an 8.6-year-old girl (patient B), who underwent subtotal transphenoidal resection followed by adjuvant PT, 5 months after initial diagnosis. MR imaging 14 months after irradiation revealed a stenosis of right internal carotid artery (Fig. 1d). The patient was however asymptomatic.

Dosimetric analysis and LETd distribution

Planning CT and MRI pre- (n=16) and post- treatment (MRI TOF 3D, *mprage* T1, T2) images [11], were used to contour the clinical volume of interest, as the OARs for vascular toxicity and PT target volumes. OARs were delineated by a senior radiation oncologist (AP) and neuro-oncologist (FA), and consisted of the circle of Willis' structures with internal carotid arteries and basilar artery. A detailed dosimetric analysis was performed and dose metrics as mean and maximum dose (for OARs) and V95% (the volume receiving at least 95% of the prescribed dose) for PTV were computed from the dose volume histograms (DVHs).

LETd distributions were computed according to Wilkens and Oelfke [12] (Appendix A) and LETd metrics (mean and maximum) for the PTV and OARs were analysed. In our

implementation, 1D LETd calculations are performed in water, considering only primary protons. Mean and maximum LETd values were calculated for all voxels within each ROI.

Range uncertainties and consequences on dose and LETd distributions

High LETd values are linked to high biological effectiveness for proton fields, especially at the end of range [10, 13] therefore small range uncertainties should be taken into account when evaluating dose distributions [14-16]. Considering the small OARs size and the dose/LETd gradients close to those structures, range uncertainties could significantly affect both dose and LETd values.

Image guidance was based on 2D-daily topograms acquired on the CT located in treatment room and compared with reference topograms acquired with the planning CT. Bite immobilisation was used for 31% of the patients' cohort, resulting in systematic and random positioning errors within 0.16 mm and 1.22 mm respectively. Five patients received anaesthesia during the treatment, thus further minimising intrafractional positioning uncertainties. Therefore, for this population, CT calibration uncertainties represent the main contribution to range uncertainties [15, 17]. This effect was simulated for a sub-cohort of patients representative of different field arrangements, including the two index cases, by introducing a +/-3% HU variation on the nominal planning CT [18] and recalculating the nominal dose. As the maximum depths of those tumours was 10.8±1.7 cm (range 7.8-13.4 cm), this translated in range errors of 0.32±0.05 cm. Additionally, based on the recalculated dose distributions, the nominal LETd distributions ($LETd_N$) were recomputed, thus obtaining new LETd distributions with simulated range error ($LETd_{RE}$). Nominal doses and LETd metrics were compared to the values obtained assuming ± 3% HU variations.

Dose–volume parameters derived from dose and LETd distributions were evaluated with the Kruskal-Wallis non-parametric test, to compare the results for the index patients vs the non-RICVs ones. A p-value <0.05 considered statistically significant.

Results

After 9.5 months' follow up (range: 14.0-75.0), tumours' volume decreased for 3 (18.8%) patients and remained stable for 13 (81.2%) other patients. No tumor progression or other non-vascular toxicities were observed during the follow-up. One patient with visual defect prior to PT had improved visual function post-treatment, whereas three patients with partial visual defects prior to PT had functional decline. The estimated 3-year vision preservation rate was 92.8%. The 3-year survival without new anterior pituitary deficit was 77.3%.

For our patient cohort, the prescribed dose of 54 Gy(RBE) did not exceed tolerance doses for the optical structures or brainstem, therefore Single Field Uniform Dose (SFUD) technique was used for 13/16 patients (81%), whilst for the remaining three patients (19%) Intensity Modulated Proton Therapy (IMPT) technique was applied [19]. Multiple fields plans (range: 2-4) with either symmetric (S, including at least one contralateral field) or asymmetric (A, no contralateral fields) were used for all the cases. In this cohort, three (19%) had asymmetric fields, of which two (67%) presented with RICVs.

Quantitative dosimetric results, based on the DVH metrics for PTV and OARs, did not reveal any evident dose metric/toxicity correlation (Table1).

For OARs, often located in high dose gradients, average dose values, were analysed and reported. No significant differences between the index cases and the non-RICV patients were

found for either mean OAR dose or PTV size. The largest PTV volume was however found for one of the index patients. Target coverage (V95% in PTV) was comparable among all patients.

The results of the LETd metric analysis for PTV and OARs are shown in Table 2, where p-values are reported concerning the differences of (i) index cases vs. non-RICV patients and (ii) asymmetric vs symmetric field arrangements.

Maximum LETd values for vascular structures are up to 7.9 keV/µm (vasculature left, patient A) and 7.7 keV/µm (vasculature right, patient B), who both presented with toxicity on the left and right side respectively. These values (see Fig. 2a), as well as the average LETd in the OAR, and maximum LETd in the PTV, were significantly higher than the ones for the rest of the population. As reported in Fig 2b and Fig 2c, for the index cases, the high maximum/mean LETd values are combined with high mean dose values in the vascular structures. Two non-RICV patients (pt C and D) presented with maximum LETd values > 5.5 keV/µm in the vascular structures, but with mean dose well below prescription (<45 Gy(RBE)). Finally, figure 2c shows that, although the combination of mean dose *and* mean LETd separate the index cases from the rest, the separation is not a clearly defined as for the combination of mean dose and maximum LETd.

The three patients treated with asymmetric fields had significantly higher ($p<0.002$, $p<0.01$) maximum LETd values in the PTV and OARs, compared to patients treated with symmetric fields (Fig. 2, Table2). For one of these patients (patient D), OAR maximum LETd was above 7keV/µm, thus comparable to index patients' values, but had a mean dose < 42Gy(RBE).

For asymmetric plans the high LETd area is also localized asymmetrically at the distal range of the lateral fields, involving the side of the Willis' structure with toxicity. For symmetric plans instead, high LETd areas are localized anteriorly and posteriorly outside the PTV (Fig. 3).

The effect of range uncertainties in mean dose and in maximum LETd values to OARs (ΔLETd between $LETd_N$ and $LETd_{RE}$ metric values), are shown in Supplemental Table 1 for 4 patients who were selected as representative of the asymmetric (patient A and B) and symmetric (patient C and E) approaches. The OAR mean dose differences , due to 3% HU variations, are slightly higher for the index patients as compared to the non-RICVs patients. Nevertheless, the maximum estimated increase of the OARs mean dose for the index patients would result in values well within the average.

The differences due to 3% HU variation in maximum OARs LETd are up to 1.2keV/μm (15%) for asymmetric arrangement, and only up to 0.7keV/μm (12%) for the symmetric one. Additionally, even assuming a decreased $LETd_{RE}$ in the OARs for the index patients (Supplemental Table1) the difference between maximum LETd values for index cases vs non-RICV patients would still be significant (p=0.02). $LETd_N$ and $LETd_{RE}$ distributions for the four patients included in the LETd range uncertainty analysis are depicted in Fig. 4.

Discussion

In this study we investigated dose and LETd distributions for 16 CP patients treated with proton PBS at PSI, between 2008 and 2014. Two of them (12.5%), showed RICVs 1.2 and 2 years after PT. Wang et al reviewed reported 77 cases of delayed RICV. The median interval period for moyamoya cases was 3.3 years (range 0.3-20, p<0.001) with photons [20]. The circle of Willis is a critical organ at risk for cerebral vascular accidents (CVA) after cranial RT. With a median follow up of 26 years, relative risk of CVA was 15.7% with ≥ 40 Gy(RBE) to the circle of Willis [21]. Large vessel cerebral vasculopathy after PT in paediatric patients seems

to occur earlier according the literature. Kralik et al [22] reported the median time from completion of RT to development was 1.5 years (mean, 3.0 years; range, 1.0-7.5 years). Hall et al [23] found in 644 pediatric patients, with a median follow up of 3.0 years (range, 0.1-9.6 years), a 3-years cumulative rate of serious vasculopathy of 2.6%. In this study major vessels were specifically contoured as OARs. In our analysis, no correlation was observed between dose distributions in the vascular structures and toxicity, therefore the analysis was extended to LETd distributions (maximum and mean values). For this, we have used maximum LETd as a metric. Although this strongly depends on the calculation grid, the use of more common surrogates of maximum dose, such as D2 would have a similar problem, due to the small OAR volume where 1 voxel equals about 1% of the volume.

In our analysis patients with RICVs (patient A and B), present with the highest maximum LETd values in the PTV (Table 2) (> 5.5keV/µm). Moreover, they also have the highest maximum LETd value, of 7.9keV/µm (vasculature left) and 7.7keV/µm (vasculature right), respectively, in the anatomical area of the observed toxicity. These values are larger than the average of the maximum LETd values for the non- RICV patients (7.8keV/µm and 4.8keV/µm respectively). Nevertheless, two non-RICV patients presented with LETd values > 7 keV/µm (ptD) and 5.5 keV/µm (ptC) in the vascular structures. As shown in Figure2b the index patients presented with the combination of both high maximum LETd *and* mean dose in the vascular structures (maximum LETd>7 keV/µm and mean dose>45 Gy(RBE)). One explanation of this could be that the 'circle of Willis' has a strong volume effect, meaning that its tolerance to localized high LETd regions is compromised (lowered) when a large volume of the structure is irradiated, even if high LETd region does not correspond to high dose region.

Similar LETd evaluation have been performed previously by Giantsoudi et al. [24], who reviewed 111 consecutive patients treated with PT for medulloblastoma between 2002 and 2011 including 10 selected patients with clinical symptoms of CNS injury. No correlation was found between the sites of injury and elevated RBE.

Sethi et al. [25] also evaluated 109 medulloblastoma patients treated with PT, aiming at correlating lower LETd values with recurrences. Eleven patients (10%) experienced relapse isolated to a single compartment, but no correlation was found between LETd distribution and region of recurrence.

An important limitation of our study is the availability of MR imaging data to accurately contour the circle of Willis structures. Ideally, the most adequate pre- and post-treatment MRI sequence for contouring such structures is an axial 3D time of flight [26], available only for a few (n=2) patients.

Target volumes were delineated using CT images co-registrated with T1- and T2- weighted post-contrast thin-sliced (1 to 1.5mm slice thickness) MRI. The GTV included solid and cystic components and has historically been expanded by a 10 mm margin to create the CTV. Recently, we used a 5 mm CTV margin adapted to anatomical barriers according to the recent phase II protocol which prospectively evaluated a 5mm CTV margin using PT with promising results in term of disease control and reduced toxicity [27].

The LETd model that was used in this study (unrestricted 1D LETd to water considering primary protons only) neglected the contribution of the secondary protons. As described in [28], the main contribution of those secondary protons is in the penumbra of the plateau region, decreasing toward the peak of the dose distribution. Therefore, their contribution at the end of the range would have only limited influence on OAR maximum LETd.

For this analysis RBE-weighted dose would be the appropriate parameter to describe the effect of dose and its radio-biological effect but, due to the complexity of RBE problem, there is no clinically validated reliable RBE model to be used [29]. Considering this, Unkelbach et al. in 2016 [30] introduced the use of a combined parameter defined as LETxD (product of LETd and physical dose), with the main purpose of including the increase of biological dose caused by high LETd in the dose optimisation. As this quantity is not yet validated, we have here instead evaluated physical doses and LETd distributions as two separate parameters.

Treatment approach (A or S) influences maximum LETd values in the vascular structures; this is instead not the case for IMPT vs SFUD. The highest LETd maximum values are for three patients (A, B, and D; Table 2) all treated with asymmetric arrangement. Patient D is even more an outlier as it presents with high maximum LETd values (>7 keV/µm) in both vascular structures (Fig. B1). This result can be interpreted as an indication to use symmetric fields, even if asymmetric fields can reduce the dose bath in the contralateral brain. However, it is dosimetrically less robust than the symmetric one, and may deliver higher LETd radiation. This has been confirmed by the LETd robustness analysis on selected cases with variations of maximum LETd below 0.7 keV/µm in case of symmetric, as compared to values below 1.2 keV/µm in case of asymmetric arrangement.

No clear correlation was found between toxicity and high maximum LETd of the basilar artery (not reported).

In summary, our dosimetric analysis could not objectivize a correlation between dose and RICV, whilst the combination of high maximum/average LETd values in the vascular structures and high mean dose seems to correlate with RICVs. Of note, both index cases had large PTVs. Asymmetric fields were associated with high LETd values, and two of the three patients

treated with this arrangement presented with RICVs, as opposed to none of those treated with symmetrical fields. As such, we are currently treating all CP patients with a symmetrical beam arrangement to potentially limit the likelihood to induce a RICV. This comes however at the cost of an increased integral brain dose and future prospective studies, including neuro-cognitive testing, should better define the optimal therapeutic ration of using asymmetrical vs. symmetrical field arrangement for CP patients.

References

[1] Omura M, Aida N, Sekido K, Kakehi M, Matsubara S. Large intracranial vessel occlusive vasculopathy after radiation therapy in children: clinical features and usefulness of magnetic resonance imaging. Int J Radiat Oncol Biol Phys. 1997;38:241-9.
[2] Cappelli C, Grill J, Raquin M, Pierre-Kahn A, Lellouch-Tubiana A, Terrier-Lacombe MJ, et al. Long-term follow up of 69 patients treated for optic pathway tumours before the chemotherapy era. Arch Dis Child. 1998;79:334-8.
[3] Brant-Zawadzki M, Anderson M, DeArmond SJ, Conley FK, Jahnke RW. Radiation-induced large intracranial vessel occlusive vasculopathy. AJR Am J Roentgenol. 1980;134:51-5.
[4] Bitzer M, Topka H. Progressive cerebral occlusive disease after radiation therapy. Stroke. 1995;26:131-6.
[5] Tanaka Y, Takeuchi K, Ogashiwa M, Akai K, Omata K. [Moyamoya phenomenon combined with cerebral aneurysm (author's transl)]. No To Shinkei. 1978;30:687-95.
[6] Desai SS, Paulino AC, Mai WY, Teh BS. Radiation-induced moyamoya syndrome. Int J Radiat Oncol Biol Phys. 2006;65:1222-7.
[7] Partap S. Stroke and cerebrovascular complications in childhood cancer survivors. Semin Pediatr Neurol. 2012;19:18-24.
[8] Strenger V, Sovinz P, Lackner H, Dornbusch HJ, Lingitz H, Eder HG, et al. Intracerebral cavernous hemangioma after cranial irradiation in childhood. Incidence and risk factors. Strahlenther Onkol. 2008;184:276-80.
[9] Passos J, Nzwalo H, Valente M, Marques J, Azevedo A, Netto E, et al. Microbleeds and cavernomas after radiotherapy for paediatric primary brain tumours. J Neurol Sci. 2017;372:413-6.
[10] Paganetti H. Relative biological effectiveness (RBE) values for proton beam therapy. Variations as a function of biological endpoint, dose, and linear energy transfer. Phys Med Biol. 2014;59:R419-72.
[11] A Lania AS, G Lasio. Diagnosis and Management of Craniopharyngiomas. 2016.
[12] Wilkens JJ, Oelfke U. A phenomenological model for the relative biological effectiveness in therapeutic proton beams. Phys Med Biol. 2004;49:2811-25.
[13] Mohan R, Peeler CR, Guan F, Bronk L, Cao W, Grosshans DR. Radiobiological issues in proton therapy. Acta Oncol. 2017;56:1367-73.
[14] Albertini F, Bolsi A, Lomax AJ, Rutz HP, Timmerman B, Goitein G. Sensitivity of intensity modulated proton therapy plans to changes in patient weight. Radiother Oncol. 2008;86:187-94.
[15] Lomax AJ. Intensity modulated proton therapy and its sensitivity to treatment uncertainties 2: the potential effects of inter-fraction and inter-field motions. Phys Med Biol. 2008;53:1043-56.
[16] Carabe A, Moteabbed M, Depauw N, Schuemann J, Paganetti H. Range uncertainty in proton therapy due to variable biological effectiveness. Phys Med Biol. 2012;57:1159-72.
[17] Schaffner B, Pedroni E, Lomax A. Dose calculation models for proton treatment planning using a dynamic beam delivery system: an attempt to include density heterogeneity effects in the analytical dose calculation. Phys Med Biol. 1999;44:27-41.
[18] Moyers MF, Sardesai M, Sun S, Miller DW. Ion stopping powers and CT numbers. Med Dosim. 2010;35:179-94.
[19] Lomax A. Intensity modulation methods for proton radiotherapy. Phys Med Biol. 1999;44:185-205.
[20] Wang C, Roberts KB, Bindra RS, Chiang VL, Yu JB. Delayed cerebral vasculopathy following cranial radiation therapy for pediatric tumors. Pediatr Neurol. 2014;50:549-56.
[21] El-Fayech C, Haddy N, Allodji RS, Veres C, Diop F, Kahlouche A, et al. Cerebrovascular Diseases in Childhood Cancer Survivors: Role of the Radiation Dose to Willis Circle Arteries. Int J Radiat Oncol Biol Phys. 2017;97:278-86.
[22] Kralik SF, Watson GA, Shih CS, Ho CY, Finke W, Buchsbaum J. Radiation-Induced Large Vessel Cerebral Vasculopathy in Pediatric Patients With Brain Tumors Treated With Proton Radiation Therapy. Int J Radiat Oncol Biol Phys. 2017;99:817-24.

[23] Hall MD, Bradley JA, Rotondo RL, Hanel R, Shah C, Morris CG, et al. Risk of Radiation Vasculopathy and Stroke in Pediatric Patients Treated With Proton Therapy for Brain and Skull Base Tumors. Int J Radiat Oncol Biol Phys. 2018;101:854-9.
[24] Giantsoudi D, Sethi RV, Yeap BY, Eaton BR, Ebb DH, Caruso PA, et al. Incidence of CNS Injury for a Cohort of 111 Patients Treated With Proton Therapy for Medulloblastoma: LET and RBE Associations for Areas of Injury. Int J Radiat Oncol Biol Phys. 2016;95:287-96.
[25] Sethi RV, Giantsoudi D, Raiford M, Malhi I, Niemierko A, Rapalino O, et al. Patterns of failure after proton therapy in medulloblastoma; linear energy transfer distributions and relative biological effectiveness associations for relapses. Int J Radiat Oncol Biol Phys. 2014;88:655-63.
[26] Scoccianti S, Detti B, Gadda D, Greto D, Furfaro I, Meacci F, et al. Organs at risk in the brain and their dose-constraints in adults and in children: a radiation oncologist's guide for delineation in everyday practice. Radiother Oncol. 2015;114:230-8.
[27] Merchant TEHC, Sabin ND, Madey MA, Wu s, Li Y, Klimo P, Boop FA, Aldana PR, Indelicato DJ. Progression-Free Survival after Proton Therapy for Childhood Craniopharyngioma: Early Results From a Prospective Trial. International Journal of Radiation Oncology*Biology*Physics. 2017;Volume 99:S59.
[28] Grassberger C, Paganetti H. Elevated LET components in clinical proton beams. Phys Med Biol. 2011;56:6677-91.
[29] Paganetti H, Giantsoudi D. Relative Biological Effectiveness Uncertainties and Implications for Beam Arrangements and Dose Constraints in Proton Therapy. Semin Radiat Oncol. 2018;28:256-63.
[30] Unkelbach J, Botas P, Giantsoudi D, Gorissen BL, Paganetti H. Reoptimization of Intensity Modulated Proton Therapy Plans Based on Linear Energy Transfer. Int J Radiat Oncol Biol Phys. 2016;96:1097-106.

Legends:

Fig. 1. Multifocal vasculopathy in the region of the circle of Willis (yellow arrows). (a) Coronal Maximum Intensity Projection (MIP) angiogram of the index patient A 24 months after PT; (b) T1-weighted MPRAGE sagittal image showing bright signal intensity (red arrowhead) with a cystic component in the suprasellar region. (c) Stenosis of the right internal carotid (arrow) for index patient B visible on the Coronal Maximum Intensity Projection (MIP) angiogram 14 months after PT.(d) T1-weighted MPRAGE coronal image showing bright signal intensity (arrowhead) in the right suprasellar region

Fig. 2. a) Maximum LETd values for the vascular structures right and left for all the patients. In red the values for the structures presenting with toxicity. The continuous lines represent the average of the maximum LETd values for vascular structures presenting with toxicities (pt A-left and pt B right) and for the rest of the population (shadow area is the standard deviation). The first three patients (A, B and D) are the ones with asymmetric field arrangements. b) Maximum LETd values vs mean dose for the vascular structures right and left for all the patients. In red the values for the structures presenting with toxicity. Toxicities present with both the highest mean doses and maximum LETd values. For the patient D, the third one with asymmetric field arrangement, high maximum LETd values are combined with mean doses in the vascular structures <42 Gy(RBE). c) Mean LETd values vs mean dose for the vascular structures right and left for all the patients. In red the values for the structures presenting with toxicity. Toxicities present with both the highest mean doses and mean LETd values (>48 Gy(RBE)). For the patient D, the third one with asymmetric field arrangement,

only one vascular structure present with mean LETd > 3.5 keV/μm , but the mean doses in the vascular structures are <42 Gy(RBE).

Fig. 3. Dose distribution and LETd distributions for patient A, C and E. Patient A has a 3 -non contralateral fields arrangement while patient C and E have a 2- contralateral fields arrangement respectively (Yellow arrows indicate field directions, if dotted they indicate non coplanar fields). High LETd areas are located close to the circle of Willis 'structures only for the non contralateral fields arrangement. The contour for the vascular structures of the circle of Willis are shown in green (arrow). For patient A T1-weighted MPRAGE axial image showing a vasculopathy in the region of the circle of Willis (green arrow).

Fig 4. – $LETd_N$ and the $LETd_{RE}$ distribution for patient A, B, C and E (from left to tight). In the central line are shown the nominal LETd distributions on the planning CTs. On the top the $LETd_{RE}$ distributions on the CTs with a HU increases of 3%. On the bottom the $LETd_{RE}$ distributions on the CTs with a HU decreases of 3%. PTV is highlighted in yellow, the circle of Willis' structures in green.

Fig B1 – Patient A (left) and D (right). The shape of the vasculature (highlighted in green), in case of the patient D explains how the LETd is high in the left vascular structure (right on the screen) despite the asymmetric field arrangement.

Table 1. Field arrangement, number of fields and dose metrics (V95% of the PTV, mean dose (%) to Circle of Willis structures) for all the patients included in the study. The values for RICV

patients are in italic. No significant differences are found for those parameters between index patients and rest of the cohort.

Table 2. Maximum and mean values of dose average LET (LETd) for PTV and vascular structures for all the 16 patients. P-values of the differences are reported considering: (i) patients with toxicity vs the rest of the cohort; (ii) patients treated with asymmetric (A) field arrangement vs patients treated with symmetric field arrangement (S) (in bold and red the significant differences). The values for RICV patients are in italic.

Supplemental Table 1. Dosimetric robustness of mean dose to OARs and LETd robustness of max LETd values to OARs. Those values are calculated modifying the HU values of the planning CT of ± 3%, to simulate a range error.

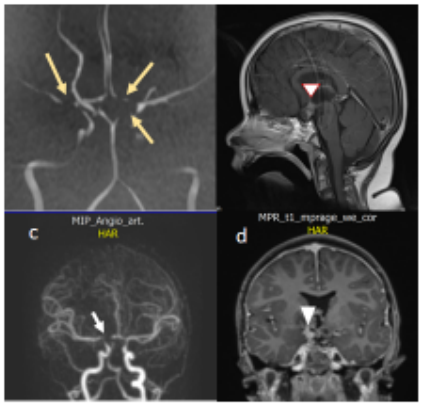

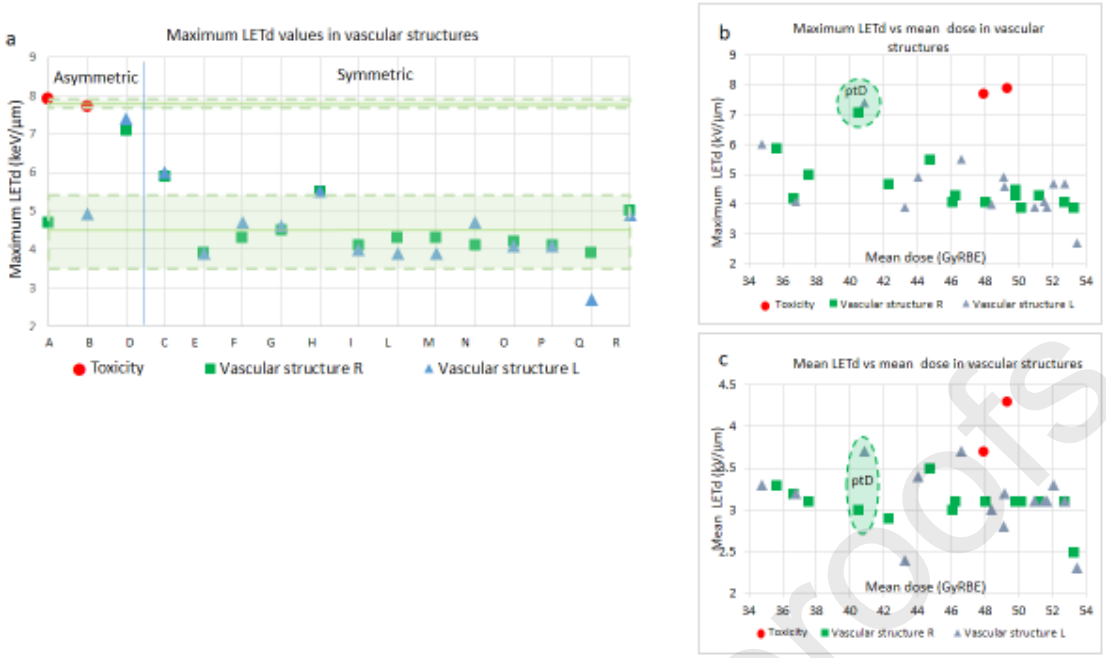

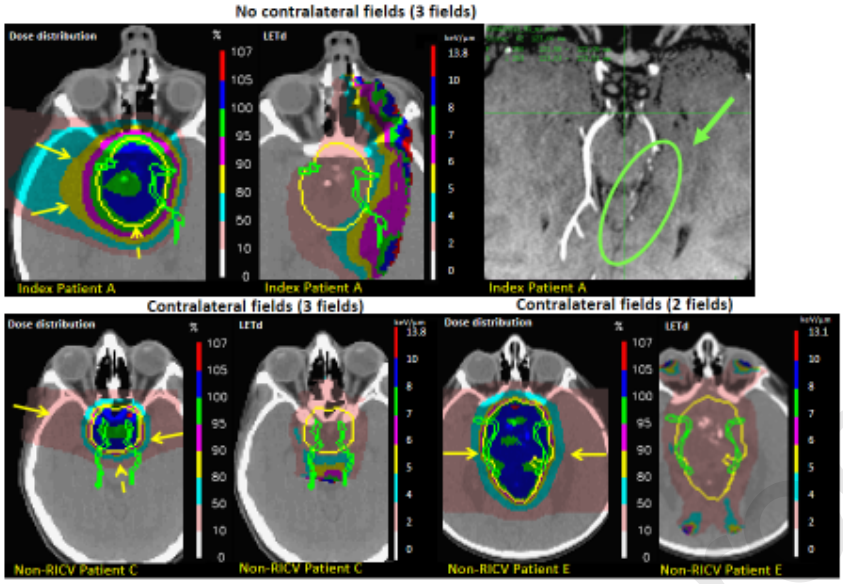

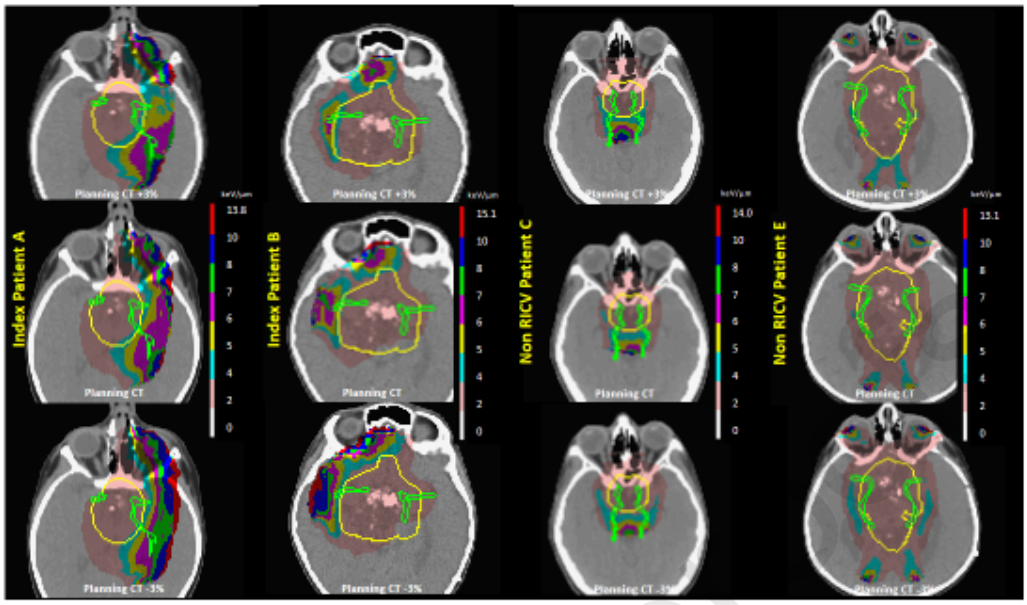

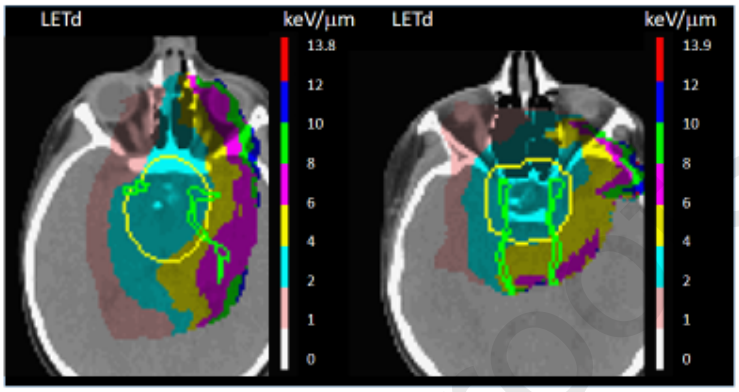

Table 1.

Patient #	Fields' arrangement	Fields' number	PTV coverage V95 (%)	PTV volume (cm^3)	Vascular R Mean dose(%)	Vascular L Mean dose(%)	Basilar art. Mean dose (%)
A-TOX	*A*	*3*	*92.7*	*62.4*	*78.2*	***91.3****	*61.4*
B-TOX	*A*	*3*	*95.7*	*159.81*	***88.7****	*90.9*	*100*
C	S	3	92.0	24.81	65.9	64.4	69.9
D	A	3	92.7	36.98	74.9	75.6	100.1
E	S	2	93.4	105.7	92.8	94.3	94.6
F	S	4	92.1	110.69	94.7	97.6	80.1
G	S	2	93.2	44.35	92.2	91	49.8
H	S	3	93.3	41.74	82.8	86.3	44.6
I	S	2	94.4	36.7	88.9	89.6	91.4
L	S	2	90.5	32.1	85.5	95.7	64.5
M	S	2	94.7	37.54	92.2	80.1	95.3
N	S	3	92.1	69.69	97.5	96.4	97.5
O	S	2	94.8	18.84	67.8	68.1	76.9
P	S	2	95.5	52.45	85.2	95.4	99.3
Q	S	3	93.6	105.18	98.6	99	93.5
R	S	2	89.9	11.63	69.4	81.5	90.2

	Fields' number	**PTV V95(%)**	**PTV (cm^3)**	**Vascular structures (mean, %)**	**Basilar art. (mean,%)**
mean ± SD	2.6±0.6	93±1.6	59±41	85±15	82±19
mean (RICV) ± SD	3	94±2.2	111±69	87±15	81±27
mean (non RICV) ± SD	2.5±0.6	93±1.7	52±42	86±6	82±18
p value		0.38	0.11	0.88	0.88
mean (A) ± SD	3	94±1.8	86±64	83±8	87±22
mean (S) ± SD	2.5±0.7	93±1.7	53±34	85±11	81±18
p value		0.64	0.31	0.23	0.25

Abbreviations: A: asymmetric field arrangement; S: symmetric field arrangement; RICV: Radiation-induced cerebral vasculopathy (RICV); TOX: index case with RICV; PTV: planning target volume; mean as % of the prescribed dose

*OAR with RICV

Table 2.

Patient #	Fields' arrangement	LETd PTV (keV/µm)		LETd Vascular R (keV/µm)		LETd Vascular L (keV/µm)	
		Maximum	Mean	Maximum	Mean	Maximum	Mean
A-TOX	*A*	*5.5*	*2.9*	*4.7*	*2.9*	***7.9****	***4.3****
B-TOX	*A*	*5.3*	*2.6*	***7.7****	***3.7****	*4.9*	*2.8*
C	S	4.6	3	5.9	3.3	6	3.3
D	A	5.1	3.1	7.1	3	7.4	3.7
E	S	4	2.7	3.9	3.1	3.9	3.1
F	S	4.4	2.9	4.3	3.1	4.7	3.1
G	S	4.2	3.1	4.5	3.1	4.6	3.2
H	S	4.1	3.1	5.5	3.5	5.5	3.7
I	S	4.1	3.2	4.1	3.1	4	3
L	S	4.4	3.3	4.3	3.1	3.9	3.1
M	S	4.3	3.1	4.3	3.1	3.9	2.4
N	S	4.9	3	4.1	3.1	4.7	3.3
O	S	4.1	3.3	4.2	3.2	4.1	3.2
P	S	4.4	2.9	4.1	3	4.1	3.1
Q	S	4.5	2.6	3.9	2.5	2.7	2.3
R	S	4.2	3.4	5	3.1	4.9	3.4

LETd values	**PTV**		**Vascular structures**	
(keV/µm)	**Maximum**	**Mean**	**Maximum**	**Mean**
mean ± SD	4.5±0.5	3.0±0.2	4.8±1.2	3.2±0.4
mean (RICV) ± SD	5.4±0.1	2.8±0.2	7.8±0.1	4.0±0.4
mean (non RICV) ± SD	4.4±0.3	3.1±0.2	4.6±1.0	3.1±0.3
p value	**0.02**	0.09	**0.02**	**0.02**
mean (A) ± SD	5.3±0.2	2.9±0.3	6.5±1.3	3.4±0.5
mean (S) ± SD	4.3±0.3	3.0±0.2	4.3±0.6	3.1±0.3
p value	**0.01**	0.12	**0.002**	0.65

Abbreviations: LETd: dose averaged Linear Energy Transfer; RICV: Radiation-induced cerebral vasculopathy (RICV); TOX: index case with RICV; PTV: planning target volume

*OAR with RICV

Highlights

- Vascular toxicity in craniopharyngioma pediatric cases after proton therapy was evaluated considering dosimetry and LET
- Two cases out of 16 pediatric patients presented with RICV.
- Vascular toxicity was found only for patients treated with asymmetric field arrangements
- High max and average LET values were found for vascular toxicity areas identified on MRI for patients with RICV.